Shape Optimization for Passive Mid-IR Photonic Components

A. Glière
Univ. Grenoble Alpes
CEA, LETI
Grenoble, France
alain.gliere@cea.fr

N. Lebbe
Univ. Grenoble Alpes
CEA, LETI
Grenoble, France
nicolas.lebbe@cea.fr

K. Hassan
Univ. Grenoble Alpes
CEA, LETI
Grenoble, France
karim.hassan@cea.fr

C. Dapogny
Univ. Grenoble Alpes
CNRS, Grenoble INP, LJK
Grenoble, France
charles.dapogny@imag.fr

E. Oudet
Univ. Grenoble Alpes
CNRS, Grenoble INP, LJK
Grenoble, France
edouard.oudet@imag.fr

***Abstract*—Shape optimization techniques were first developed in the context of mechanical engineering and, quite recently, applied to photonic components for data communication. Here, motivated by the growing application potential of mid-IR photonics driven by chemical sensing and spectroscopy, we present the design by shape optimization of passive components operating in this wavelength range.**

Keywords—shape optimization, level-set, mid-IR photonics

I. Introduction

Driven by data communication in the near-IR wavelength range, silicon photonics has experienced tremendous developments in the last few decades. The transposition of this scientific and industrial success to the mid-IR (3 µm to 12 µm) has been envisioned some time ago [1] and is currently under rapid progress, with noteworthy developments in materials, passive and active components, laser sources, photodetectors and sensors [2]. Due to the strong absorption bands situated in this wavelength range, notable applications are found in trace gas sensing, spectroscopy and imaging of biological tissues.

The founding principles of shape optimization can be traced back to I. Newton who aimed at minimizing the drag force exerted over a moving body. Since then, numerous mathematical developments have occurred and shape optimization, further boosted by additive manufacturing technologies, has been successfully applied in structural mechanics [3]. More recently, shape optimization appeared in the domain of silicon photonics, first with simulations and designs of passive devices [4][5] and then with micro fabrication and experimental demonstrations [6]. However, to our knowledge, only data communication oriented devices, that is components functioning in the near-IR have been investigated.

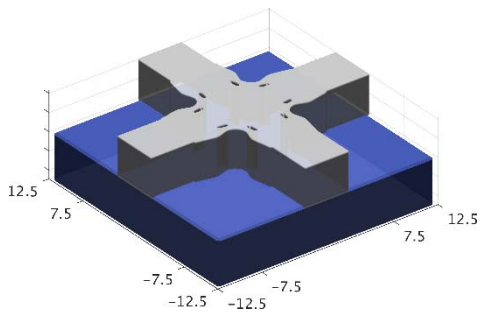

Fig. 1. The mid-IR platform is composed of 4.6 µm thick SiGe waveguides (grey) etched on a silicon substrate (blue). Dimensions are in µm.

The scope of this paper is thus to demonstrate the capabilities of shape optimization techniques in the mid-IR range. After a brief description of the model used to solve the direct electromagnetic problem and a summary of our shape derivative-based optimization technique, we present a few passive components designed for operation in the mid-IR.

II. Photonic Model

A. The technological platform

The semiconductor platform used as a basis for our design work is composed of a SiGe alloy layer, chosen for its transparency up to the wavelength of 8 µm, deposited on a silicon substrate. The waveguides and photonic building blocks are fully etched in this 4.6 µm thick SiGe layer and are surrounded with air (Fig. 1).

A quantum cascade laser provides the light injected in the circuit at the wavelength of 7.4 µm in the TM polarization.

The values of the optical indices used for the computations are 3.54 for the $Si_{60\ \%}Ge_{40\ \%}$ alloy and 3.42 for the silicon substrate. In these conditions, 5 µm x 4.6 µm cross-section waveguides support a single TM guided modes (the second TM mode appears above the width of 9.7 µm).

B. Maxwell equations and boundary conditions

Assuming that all materials are linear, isotropic and non-dispersive dielectric with optical index n and that all sources are time harmonic with pulsation ω, the complete set of Maxwell equations reduces to two decoupled wave equations, respectively for the electric field $\boldsymbol{E}$ and magnetic field $\boldsymbol{H}$. In fact, the solution of only one wave equation, for instance that for the electric field

$$\nabla \times \nabla \times \boldsymbol{E} - k^2 n^2 \boldsymbol{E} = 0 \text{ with } k = \omega/c \qquad (1)$$

is required and the other field, can be derived easily afterwards from the relevant Maxwell equation.

Two types of boundary conditions are applicable to our problems, namely mode injection boundary condition on the waveguide entrance face and perfectly matched layers on all other faces of the domain.

III. Shape Optimization

Shape optimization is an inverse methodology that consists in determining the distribution of materials in a domain that fulfills a given objective. For example, in the two

examples presented hereunder, the material distribution, and thus the optical index distribution, is chosen to either maximize the transmission through a waveguide crossing (Fig. 2) or to equally split the power density injected in an input waveguide between two output waveguides (Fig. 3).

Our approach [7] differs from the generally used ones in that, instead of optimizing for a continuous optical index density, possibly penalized, such as in the popular SIMP method [4], we rely on a geometrical representation of the shape, preserving binary valued indices (n_{SiGe} or n_{air}).

The shape is defined by the zero contour of a level-set function. It is optimized by a gradient descent algorithm advecting the level-set along its normal on a distance determined by the means of a formal calculation of the shape derivative [3]. The expression of the shape derivative also relies on the numerical solution of an adjoint problem accounting for the objective of the optimization.

The three-dimensional solution of the direct (1) and the adjoint problems are performed by the means of the finite element method, as implemented in the COMSOL Multiphysics commercial software (COMSOL AB, Stockholm, Sweden). The global algorithm, as well as the advection of the level-set are implemented in MATLAB (The MathWorks Inc., Natick, U.S.A.).

IV. Results

The methodology presented above has been applied to two test cases, namely a compact waveguide crossing and a compact power splitter.

In the first test case (Fig. 2), light is injected in the first TM mode in the left guide and transmission in the same mode through the crossing is maximized. The shape evolves in the 15 µm × 15 µm dashed square, from initial conditions consisting in a plain cross, to a converged one after 100 iterations. Around 93 % of the power is transmitted. Let us note that the size of the voids (~ 0.6 µm) is *a priori* compatible with the overall resolution of our fabrication process.

In the power splitter test case (Fig. 3), light is injected in the first TM mode in the lower guide and a 50 % transmission in the same mode in each of the top waveguides is expected. The shape evolves in the 20 µm × 20 µm dashed square, from initial conditions consisting in a hollow semi-circle, to a converged one after several hundred iterations. Only 37 % of the power is transmitted in each exit guide.

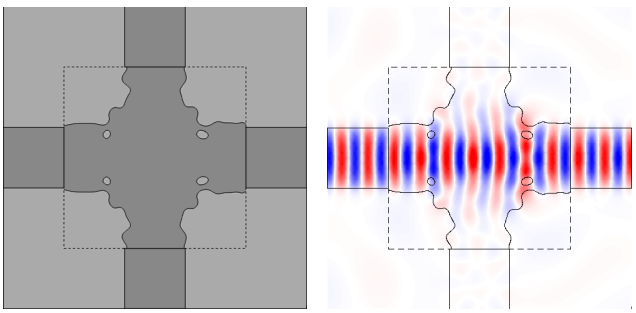

Fig. 2. Shape optimized waveguide crossing (left) and normal component of the electric field (right). The optimization domain lies in the dashed line square (15 µm × 15 µm).

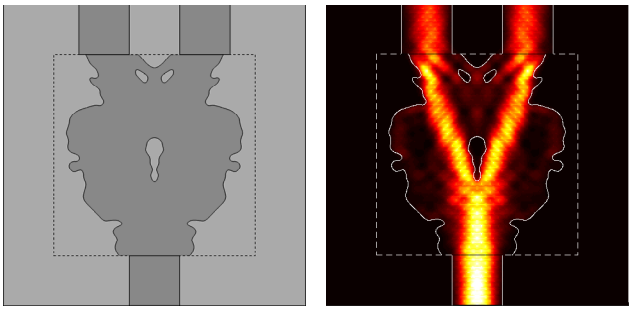

Fig. 3. Shape optimized power splitter (left) and energy density map (right). The side of the dashed line square measures 20 µm.

Performances closer to our 50 % goal could probably be obtained by testing different initial conditions or size of the shape optimization domain but the low index contrast between the silicon substrate and the SiGe layer probably limits the efficiency of the guiding structure. Let us note however that, at this wavelength and on a similar semiconductor platform, conventional components fulfilling the power splitting function, such as multimode interference couplers or directional couplers would respectively span over ≥ 60 µm or ~ 300 µm.

V. Discussion and Future Work

In this paper, our mathematically sound methodology, dedicated to shape optimization of photonic components has been summarized and preliminary results in the mid-IR have been presented. To the best of our knowledge, this constitutes the first attempt to address the specific difficulties encountered in this wavelength range.

Naturally, when compared to conventional ones, the very small footprint of the shape optimized building blocks is hindered by degraded performances in terms of insertion losses. Thus, additional progress is needed to fully take advantage of their high density integration potential. Moreover, the robustness of the design obtained so far to fabrication uncertainties (dimensions, materials) is a concern and, in order to address this issue, the methodology developed in our group [7] will shortly be harnessed.

In the near future, a more comprehensive library of passive components, comprising in particular wavelength duplexers and mode converters, will be developed and the fabrication and tests in the CEA-LETI facilities will be undertaken.

References

[1] R. Soref, "Mid-infrared photonics in silicon and germanium," *Nat. Photonics*, vol. 4, no. 8, p. 495, 2010.

[2] J. M. Fedeli and S. Nicoletti, "Mid-IR silicon-based photonics," *Proc. IEEE*, in press, 2018.

[3] G. Allaire, *Conception optimale de structures*, vol. 58. Springer Berlin Heidelberg, 2006.

[4] J. S. Jensen and O. Sigmund, "Topology optimization for nano-photonics," *Laser Photonics Rev.*, vol. 5, no. 2, pp. 308–321, Mar. 2011.

[5] J. Lu and J. Vučković, "Nanophotonic computational design," *Opt. Express*, vol. 21, no. 11, p. 13351, Jun. 2013.

[6] K. Aydin, "Integrated optics: Nanostructured silicon success," *Nat. Photonics*, vol. 9, no. 6, pp. 353–355, Jun. 2015.

[7] N. Lebbe, C. Dapogny, E. Oudet, K. Hassan, and A. Glière, "Robust shape and topology optimization of nanophotonic devices," unpublished.